

Development of a Neural Statistical Model for the Relative Humidity Levels Prediction in the Region of Rabat-Kenitra (Morocco)

Kaoutar Elazhari (✉ k.elazhari@gmail.com)

Moulay Ismail University <https://orcid.org/0000-0001-9309-0073>

Badreddine ABDALLAOUI

23 Street of Fort Neipperg

Ali DEHBI

Moulay Ismail University

Abdelaziz ABDALLAOUI

Moulay Ismail University

Hamid ZINEDDINE

Moulay Ismail University

Research Article

Keywords: Modeling, ANN, MLP, learning algorithm, Relative humidity, Rabat-Kenitra.

Posted Date: May 24th, 2021

DOI: <https://doi.org/10.21203/rs.3.rs-385467/v1>

License:   This work is licensed under a Creative Commons Attribution 4.0 International License.

[Read Full License](#)

Development of a neural statistical model for the relative humidity levels prediction in the region of Rabat-Kenitra (Morocco)

1 Kaoutar EL AZHARI¹, Badreddine ABDALLAOUI², Ali DEHBI¹, Abdelaziz
2 ABDALLAOUI¹, Hamid ZINEDDINE¹

3 ¹ Moulay Ismail University, Faculty of Science, Chemistry-Biology Applied To the
4 environment (CBAE), Analytical Chemistry and Electrochemistry, Processes and
5 Environment team, Meknes, Morocco.

6 ² 23 Street of Fort Neipperg, 2230, Luxembourg.

7 Abstract

8 This work provides the development of a powerful artificial neural network (ANN) model,
9 for the prediction of relative humidity levels, using other meteorological parameters of the
10 Rabat-Kenitra region. The treatment was applied to a database containing a daily history of five
11 meteorological parameters of 9 stations covering this region for a period from 1979 to mid-
12 2014.

13 We have shown that for the prediction of relative humidity in this region, the best performing
14 three-layer ANN (input, hidden and output) mathematical model is the multi-layer perceptron
15 (MLP) model. This neural model using the Levenberg-Marquard algorithm, having an
16 architecture [5-11-1] and the transfer functions Tansig in the hidden layer and Purelin in the
17 output layer was able to estimate values for relative humidity very close to those observed.
18 Indeed, this was affirmed by a low mean squared error (MSE) and a fairly high correlation
19 coefficient (R), compared to the statistical indicators relating to the other models developed as
20 part of this study.

21 **Key words** — Modeling; ANN; MLP, learning algorithm; Relative humidity; Rabat-
22 Kenitra.

23 **I. Introduction**

24 For a coastal zone, the problem of excessive humidity is a constant concern, especially for
25 vulnerable people, for industries such as the building industry, the pharmaceutical sector, etc.
26 In fact, Excessive moisture causes several types of allergic reactions, deterioration, mold
27 formation, rapid corrosion and mechanical damage. The limit value of humidity excessive is

28 set at 75% relative humidity. The need to control and predict variations in this environmental
29 parameter is considered as a major challenge.

30 Different scientific studies affirmed the effectiveness of networks of artificial neurons
31 (ANN) in the data processing, simulation and the modelling of the relations which control
32 correlations between environmental parameters. These neural networks have been used
33 successfully in several domains, such as the image processing, optimization, forecasting and
34 prediction in general. In fact, they are considered as information processing techniques, which
35 are established concretely by algorithms involving concepts associated with the nature of the
36 brain for the notion of learning.

37 In bibliography, we cite as examples some prediction work using, among others, MLP
38 (Multi-Layer Perceptron) artificial neural network type:

39 Parishwad and al. [**Parishwad and al., 1998**] developed mathematical models to predict
40 meteorological parameters at different locations in India such as estimating the outdoor ambient
41 temperature from relative humidity and wind speed.

42 Imran and al. [**Imran and al., 2002**] used artificial neuron networks to develop a
43 mathematical model to predict the mean values of outside ambient temperature 24 hours in
44 advance. The neural network formed was successfully tested to estimate temperatures for years.

45 Kemajou and al. [**Kemajou et al., 2012**] developed a neural model to predict the hourly
46 indoor air temperature seven hours in advance in modern buildings and in hot and humid
47 climate.

48 Turkan and al. [**Turkan et al. 2016**] predicted the average daily temperature and average
49 relative humidity in a teaching building in a hot and humid city in Turkey by applying artificial
50 neural networks. The values of the correlation coefficient obtained between the predicted values
51 and the actual values were considered by the authors to be significantly important.

52 In 2014, El Badaoui and his collaborators [**El Badaoui and al., 2014**], treated a time series
53 of meteorological data and showed the robustness of artificial neural networks of the multilayer
54 perceptron type by developing neural statistical models of the multilayer perceptron type and
55 of the radial basis function type for the prediction of the humidity rate of the city of Chefchaoun
56 in Morocco.

57 Ben El Houari and al. [Ben El Houari and al. 2014; 2015; 2016] recently developed
58 mathematical neural models for the prediction of air temperature and precipitation in the city
59 of Meknes in Morocco. They used several indices and statistical indicators to evaluate the
60 performance of their models developed and to justify the choice of learning algorithms,
61 numbers of hidden layers and neurons and activation functions.

62 Otherwise, Ben El Houari et al. [Ben El Houari and al., 2016] used the self-organizing maps
63 based on artificial neural networks to identify classes of similar objects in a database containing
64 meteorological parameters of Meknes city (Morocco). Acquired results allowed classifying the
65 216 months corresponding to the period of their study into three classes, according to the
66 meteorological parameters: A class, made up of 76 months, characterized by fairly high
67 averages of temperature, relative humidity and wind speed. A second class consisting of 56
68 months, categorized by low averages of temperature, heavy rainfall and relative humidity. A
69 third class consisting of 84 months characterized by very high temperatures and low values of
70 relative humidity, precipitation and wind speed.

71 Furthermore, and regarding relative humidity, it largely depends on many meteorological
72 parameters [Bimal and al., 2011] especially temperature: the higher the air temperature, the
73 more water vapor it can contain.

74 In the present work, our objective is to establish an efficient model based on artificial neural
75 networks to predict relative humidity in the region of Rabat-Kenitra (north-west of Morocco).
76 This prediction will take as inputs other meteorological parameters such as that the maximum
77 of temperature, minimum of temperature, precipitation, wind speed and intensity of solar
78 radiation.

79 **II. Materials and methods**

80 **II. 1 Database description**

81 The database used for this study consists of the daily values of six meteorological variables,
82 recorded between 01/01/1979 and 07/21/2014, in 9 stations installed in three parallel rows in
83 the region of Rabat-Kenitra (Morocco) (Fig. 1). Hence, 12,986 days for each station.

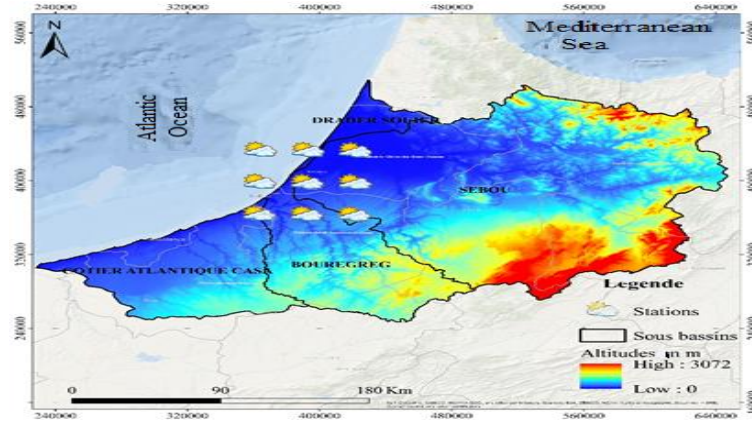


Fig. 1 : Map of meteorological stations location in the Rabat-Kenitra region (Morocco).

The six variables include:

- Five independent (explanatory) variables: maximum of temperature, minimum of temperature, precipitation, wind speed, intensity of solar radiation.
- A dependent variable (to be predicted): the humidity rate (the relative humidity).

Table 1 presents these meteorological variables, their types, their symbols, and their units. It is reported that the daily values of these variables were converted into monthly averages (i.e. 427 observations) for all variables except for precipitation, which was transformed into a monthly cumulative value, as indicated by several authors [Bishop , 1995; Dedecker and al., 2002].

Tab.1 : Meteorological parameters their symbols, their units of measurement, the notation and type of each variable.

Meteorological parameters	Symbol	Unit	Notation	Types of variable
Maximum of temperature	T_{max}	°C	X_1	Independent variables
Minimum of temperature	T_{min}	°C	X_2	
Precipitation	Pr	mm	X_3	
Wind speed	V	m/h	X_4	
Intensity of solar radiation	S	MJ/m ²	X_5	
Relative humidity	HR	%	Y	Dependent variable

II. 2 Normalization and distribution of the database:

The incompatibility of the units of measurement between the variables can affect the results. Moreover; the amplitudes of the values of the variables in the database are very different. For a good homogenization of these values, which will be propagated in the artificial neuron

101 network, the database has undergone a pre-processing, which consists in carrying out an
 102 appropriate normalization taking into account the amplitude of the values accepted by the
 103 network [Dombayc and al., 2009].

104 So, the values of the independent variables and those of the dependent variable were
 105 normalized in the interval [-1; 1], relative to their minimum and maximum values, applying the
 106 following normalization equation: [El Badaoui and al., 2014]:

$$107 \quad \bar{X}_i = \frac{2 (X_i - X_{i(min)})}{(X_{i(max)} - X_{i(min)})} - 1$$

- 108 Avec :
- 109 \bar{X}_i : Normalized values of the variable i;
 - 110 X_i : Gross values, non-normalized values of variable i;
 - 111 $X_{i(min)}$: Minimum values of variable i;
 - 112 $X_{i(max)}$: Maximum values of variable i.

113 Furthermore, in order to develop an application based on neural networks, it is necessary to
 114 divide the database into two groups: one group for training and another to test the trained
 115 network and determine its performance.

116 For it, we randomly divided our database into two groups according to well-defined
 117 percentages. Table 2 presents the values of the correlation coefficients and the mean square
 118 errors obtained for each distribution of the database and this for three different tests.

Tab.2 : Correlation coefficients (R) and mean square errors (MSE) for each database distribution.

Training group		90%	80%	70%
Validation et test group		10%	20%	30%
Test 1	R	0,82	0,83	0,92
	MSE x 10⁺⁴	0,12	0,93	0,01
Test 2	R	0,81	0,83	0,90
	MSE x 10⁺⁴	0,74	0,15	0,09
Test 3	R	0,73	0,90	0,93
	MSE x 10⁺⁴	0,41	0,67	0,08
Average of the 3 tests	R	0,79	0,85	0,92
	MSE x 10⁺⁴	0,42	0,58	0,06

120 Table results analysis indicates that the best distribution of the database is that which
121 includes 70% of the database for the training base (learning) and 30% for the validation and
122 test base). In fact, with this distribution, we obtained during the apprenticeship the most
123 important correlation coefficient and the closest to 1 ($R = 0.92$ - average of 3 tests) and the
124 lowest mean square error ($MSE = 0,06 \times 10^{-4}$ - average of 3 tests).

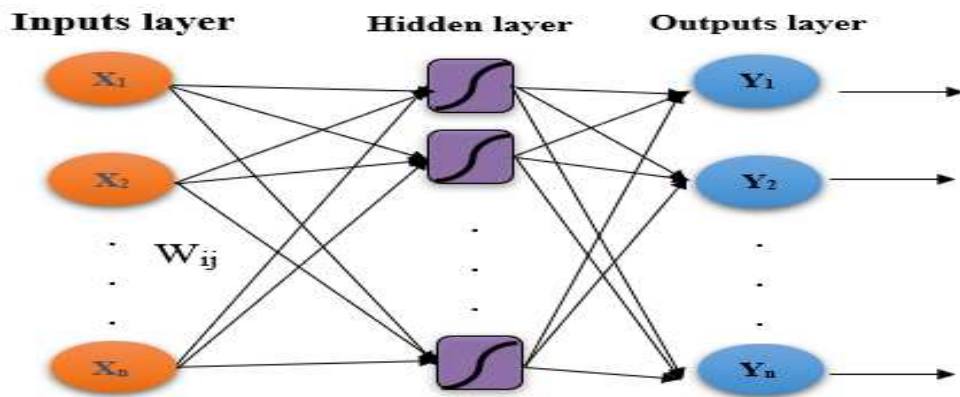
125 **II. 3 Artificial Neural Networks**

126 **II.3.1. Introduction :**

127 Through their performance in environmental modeling and simulation, artificial neural
128 networks are generally used in solving problems of a mathematical nature and precisely in
129 statistical problems where variables are linked by non-linear relationships [El Azhari and al.
130 **2017; El Badaoui and al., 2014**]. These neural networks, whose design is schematically inspired
131 by the functioning of biological neurons, have found many applications in several fields.:
132 optimization [French and al., 1992; Gardner and al., 1998], estimation [Hsu and al., 1997;
133 Hubbard and al., 2003; Imran and al., 2002] data simulation [Kemajou and al., 2012; Laafou
134 and al., 2016], environmental parameters analysis [Luk and al., 2000; Mahmood and al., 2005;
135 Omari and al., 2016] , and also in the fields of forecasts and predictions [Parishwad and al.,
136 1998; Radhika and al., 2009; Rojas R., 1996; Santhosh and al., 2010; Smith and al., 2006;
137 Turkan and al., 2012; Trahi, 2011].

138 A neuron performs a non-linear transformation between the inputs and the output. In other
139 words, a neuron performs a non-linear function of a combination of parameter-weighted X_i
140 inputs (where w_i are the weights). The linear combination is called potential (n), to which is
141 added a constant term w_0 or "bias". These networks are all composed of artificial neurons
142 connected to each other by connections [El Azhari and al., 2017; El Badaoui and al., 2014].

143 A neural network typically consists of three layers of neurons. (Fig. 2):



144
145 **Fig. 2 :** Architecture of a neural network with 3 layers.

- 146 ➤ A layer responsible for coding the information relating to the independent input
147 variables. In this layer no calculation is done.
- 148 ➤ One or more intermediate or hidden layers, where all optimization calculations of
149 neural network parameters are performed. The number of units in the middle layer is
150 determined by the user based on the reliability of the expected results.
- 151 ➤ An output layer loaded to estimate (calculate), the dependent variable (s) to predict
152 **[Gardner and al., 1998].**

153 **II.3.2. Multilayer perceptron (MLP) :**

154 The multi-layered perceptron consists of an assembly of neurons distributed over several
155 successive layers: an input layer, one or more hidden layers and an output layer. Its neurons are
156 characterized by:

- 157 ➤ Each neuron of a layer receives signals from the previous layer and transmits the result
158 to the next one, if it exists.
- 159 ➤ Neurons of the same layer are not interconnected.
- 160 ➤ A neuron can only send its result to a neuron located in a next layer.

161 For multi-layered perceptron, all or part of the neurons in a layer are connected with all or
162 part of the neurons in the adjacent layers. However, the number of hidden layers and the number
163 of neurons per layer have a significant effect on model performance.

164 **II.3.3. Statistical indices calculated**

165 To assess the performance of the different types of ANN studied; two statistical indices were
166 calculated for each type of ANN:

- 167 ✓ The correlation coefficient of Person (R), which is the square root of the coefficient
168 of determination (R²). It measures the intensity of the linear link between two
169 variables, it is given by the relation:

170
$$R = \sqrt{1 - \frac{\sum_j (\hat{Y}_j - Y_j)^2}{\sum_j (Y_j - Y_{avr})^2}}$$

171 \hat{Y}_j Estimated value j for the variable Y. Y_j : Observed j value of variable Y.

172 j varies from 1 to N. N (number of observations).

173 Y_{avr} : Average value of the variable Y calculated from the N observed values.

174

- 175 ✓ The mean squared error also called squared risk, which we will denote by MSE: it
176 represents the arithmetic mean of the squares of the deviations between the observed
177 values and the values estimated by a model.

178 The mean square error is a measure of the quality of a model; it is always positive, and
179 values closer to zero are better.

180 It is very useful for comparing several models. The most efficient model is simply the
181 one with the smallest mean square error.

182
$$MSE = \frac{1}{N} \sum_{j=1}^N (\hat{Y}_j - Y_j)^2$$

183 **III. Results and Discussion**

184 **III. 1 ANN type effect**

185 Referring essentially to the literature review, we have limited trials on six types of neural
186 networks that have been shown to be effective in similar studies (Table 3). It presents the
187 obtained values of the correlation coefficient and the mean square errors for 6 types of neural
188 networks tested.

189

Tab.3 : Values of the performance indicators according to the type of ANN.

ANN type	R	MSE x 10 ⁺⁵	Iteration
<u>Multilayer Perceptron (MLP)</u>	<u>0,99</u>	<u>4,51</u>	<u>19</u>
Feed-forward distribut time delay (FFDTD)	0,89	8,31	33
Cascade forward backprop (CFB)	0,99	4,57	21
Elman bacprop (EB)	0,83	4,90	28
Layer reccurent (LR)	0,62	5,77	25
NARX	0,49	1,42	44

190 Table 3 shows that the most effective model for predicting air humidity in the Rabat-Kenitra
 191 region is the multilayer perceptron network (MLP). Indeed, this type has a remarkably higher
 192 correlation coefficient, a lower MSE and a lower number of iterations, compared to those
 193 relating to the other types of neural networks tested.

194 **III. 2** Number of neurons in the hidden layer effect

195 To limit the calculation time and in particular when the expected results are satisfactory, a
 196 network with only one intermediate layer is used. Therefore, we tested the effect of the number
 197 of hidden neurons by varying their number from 1 to 20 neurons in the hidden layer.

198 Table 4 shows all the results relating to the values of the performance indicators according
 199 to the number of neurons in the hidden layer (HLN).

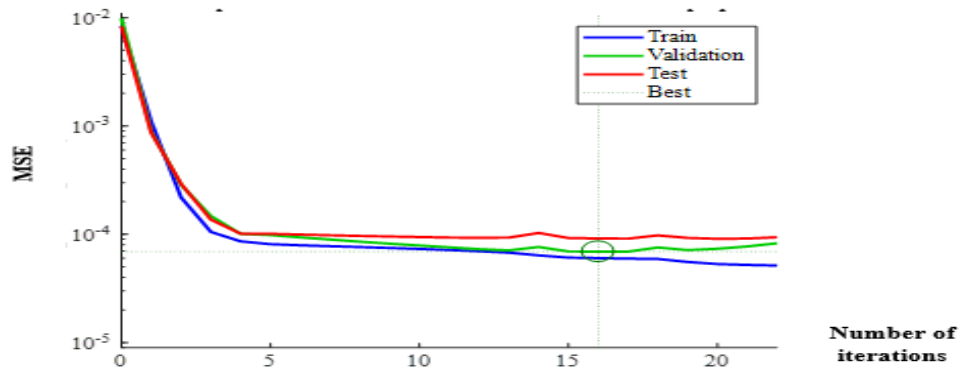
200
201

Tab.4 : Values of performance indicators as a function of the number of neurons in the hidden layer (HLN).

HLN	MSE $\times 10^{+4}$	R	Iteration
1	3,20	0,84	154
2	2,01	0,85	209
3	0,83	0,85	31
4	1,75	0,86	19
5	2,71	0,89	86
6	7,68	0,87	121
7	1,02	0,90	22
8	6,06	0,91	209
9	1,53	0,90	8
10	5,03	0,93	22
11	0,11	0,96	4
12	0,54	0,92	18
13	4,14	0,93	29
14	0,27	0,89	14
15	0,16	0,92	65
16	1,36	0,91	143
17	0,66	0,91	15
18	3,16	0,89	5
19	1,35	0,90	25
20	0,71	0,92	132

202 It is clear that the error decreases significantly when the number of neurons in the hidden
203 layer is 11 neurons (HLN = 11 neurons) since the correlation coefficient indicates a
204 convergence towards a higher and optimal value when the number of neurons in the hidden
205 layer is equal to 11. Similarly for this number of hidden neurons we recorded the largest
206 correlation coefficient (0.96), compared to those for other hidden neuron numbers, between 1
207 and 20. In addition, the learning duration (learning sequence) noted here number of iterations
208 is optimized to 4.

209 In addition, Figure 3 describes the evolution of the average quadratic error of the three phases
210 of learning (train), validation and testing with 11 neurons in the hidden layer.



211
212 **Fig. 3 :** Evolution of average quadratic error with 11 neurons in the hidden layer.

213 It shows that for the three phases the curves converge correctly, towards the minimum mean
214 square error (MSE).

215 **III. 3** Activation functions effect

216 The multilayer perceptron (PMC) uses nonlinear and linear activation functions; widely used
217 functions have the following syntax in MATLAB:

- 218 ✓ Hyperbolic tangent: Tansig ;
- 219 ✓ Sigmoid: Logsig ;
- 220 ✓ Linear: Purelin.

221 The results obtained by combining the different transfer functions in the hidden layer and
222 the output layer for the MLP model are given in table 5.

223 **Tab.5 :** Values of the performance indicators of the models developed by the MLP-type
224 neural network for different transfer functions in the hidden layer and the output layer.

Hidden layer	Output layer	R	MSE
Tansig	Tansig	0,98	1,12
Tansig	Logsig	0,93	1,18
Tansig	Purelin	0,98	0,96
Logsig	Logsig	0,93	10,65
Logsig	Tansig	0,98	0,94
Logsig	Purelin	0,92	1,21
Purelin	Purelin	0,96	3,55
Purelin	Logsig	0,96	13,02
Purelin	Tansig	0,96	3,11

225 From the analysis of the results of this table, the best performance emerges for the pair of
226 Tansig-Purelin transfer functions that is to say with a Tansig function in the hidden layer and
227 the Purelin function in the output layer. Indeed, for this pair of functions we recorded the largest
228 correlation coefficient and the lowest mean squared error.

229 **III. 4** Learning algorithm effect.

230 The performances about ten of the most efficient algorithms in the field of meteorological
231 modeling were compared for the training of predictive models. These algorithms are:

232 **III.4.1. One Step Secant (OSS) algorithm:**

233 This is a quasi-Newtonian method with the advantage of not storing the complete Hessian
234 matrix. To avoid the calculation of the inverse matrix, this One Step Secant algorithm assumes
235 that at each iteration, the preceding Hessian is the identity matrix.

236 **III.4.2. Batch gradient descent with inertial term (momentum):**

237 In most cases, if the error function has more than one local minima the network will be stuck
238 in one of them or in a region where the error surface is flat. To do this, researchers introduced
239 a momentum term α in the back propagation learning rule which acts as a low pass filter, and
240 which eliminates tiny variations on the error surface to avoid imprisonment in a local minimum.

241 **III.4.3. Conjugate gradient algorithms:**

242 The search in the methods of conjugate algorithms is done in conjugate directions instead of
243 the direction opposite to that of the gradient of the cost function. These algorithms are
244 characterized by their convergence speeds much higher than that of conventional gradient
245 algorithms [El Badaoui and al., 2014], [Laafou and al., 2016]. There are many types of
246 conjugate gradient algorithms that can be used for training such us: [El Badaoui and al., 2014]:

- 247 ✓ **Conjugate Scalar Gradient (CSG) ;**
- 248 ✓ **Gradient conjugated with Fletcher-updates Reeves (FR) ;**
- 249 ✓ **Gradient combined with Polak-Ribière (PR).**

250 **III.4.4. Resilient back propagation**

251 The Resilient back propagation algorithm is used to eliminate the harmful effects of the
252 moduli of partial derivatives, especially for neural networks using the sigmoid function as
253 transfer functions.

254 **III.4.5. Bayesian regularization-backpropagation (BR-BPNN)**

255 This learning algorithm is used to predict some aspects of the gecko spatula detachment such
 256 as the variation of the maximum normal and tangential withdrawal forces and the force angle
 257 resulting in the detachment with the peel angle.

258 **III.4.6. Random Weight/Bias Rule (NR)**

259 It generally uses some form of gradient descent method, which are known to be long,
 260 sensitive to initial parameter values, and converging to local minima.

261 **III.4.7. Levenberg-Maquardt (LM)**

262 It is an improvement of the classical Gauss-Newton numerical method in solving
 263 optimization and nonlinear least squares regression problems. The method is presented in detail
 264 by Moré in 1977. It is the recommended method for nonlinear least squares regression
 265 problems, because it is the most efficient compared to optimization algorithms.

266 We tested the performance of these algorithms. In table 6, we present the summary of these
 267 tests. It displays the values of the performance indicators of the models developed by the PMC
 268 type neuron network according to the learning algorithms studied.

269 **Tab.6 :** Values of the performance indicators of the models developed by the MLP type
 270 neural network according to the learning algorithms studied.

Learning algorithme	R	MSE x 10 ⁺⁴
One Step Secant (OSS)	0,94	0,74
Batch gradient descent with inertial term (momentum)	0,87	3,11
Gradient conjugate scalar (GCS)	0,97	2,08
Gradient conjugated with Fletcher-updates Reeves (FR)	0,96	0,35
Gradient combined with Polak-Ribière (PR)	0,97	0,20
Backpropagation (RProp)	0,97	0,22
Gradient Descent (GD)	0,88	10,35
Bayesian regularization-backpropagation (BR-BPNN)	0,96	10,16
Random Weight/Bias Rule (NR)	0,95	0,54
Levenberg-Marquardt (LM)	0,98	0,08

271 From the results, it is clear that the Levenberg Marquardt learning algorithm has the best
 272 performance. With this algorithm, we obtained the best correlation coefficient and the lowest
 273 mean squared error, in comparison with the other algorithms studied.

274 **III. 5** Summary of the best performance of the neural model

275 The results compared in Table III.9, show that the models established by the RNAs are
 276 clearly efficient whether it is for the learning or testing phase.

277 **Tab.7 :** Indices de performances obtenues par RLM pour les phases

Phases	R	MSE x 10 ⁺⁴
Learning	0.98	0.08
Test	0.96	0.21

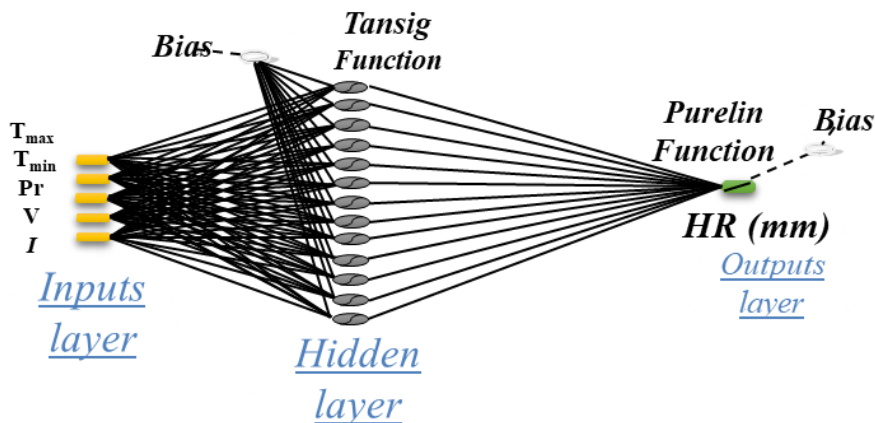
278 Correlation coefficients obtained by testing the validity of the models established by the
 279 ANNs are clearly close to those relating to learning. This shows a very good correlation between
 280 the simulated and observed values with a very good statistical indicators. This shows, the
 281 predictive advantage of these models established by artificial neural networks in predicting
 282 relative humidity levels in Rabat-Kenitra region.

283 **III. 6** Architecture and equation of the ANN model.

284 **III.6.1 Architecture of the RNA model:**

285 The most efficient network, developed for the prediction of the relative humidity of the
 286 Rabat-Kénitra region, from meteorological parameters, has a configuration [5-11-1] and
 287 therefore contains (Fig. 4):

- 288 ✓ 5 neurons in the input layer which correspond to the meteorological parameters;
- 289 ✓ 11 neurons in the hidden layer;
- 290 ✓ 1 neuron in the output layer which corresponds to the rate of relative humidity.



291 **Fig. 4 :** Architecture of the neural network with three configuration layers [5-11-1] developed for
 292 the prediction of relative humidity in the region of Rabat-Kenitra.
 293

294 **III.6.2 Equation obtained with the ANN model:**

295 Then, the equation obtained by the most efficient PMC type RNA model of configuration

296 [5-11-1] is:

$$297 \quad Y = \text{Purelin} \left(\text{LW}_{2,1} \left(\text{Tansig} \left(\text{IW}_{1,1} * X + \theta_1 \right) \right) + \theta_2 \right)$$

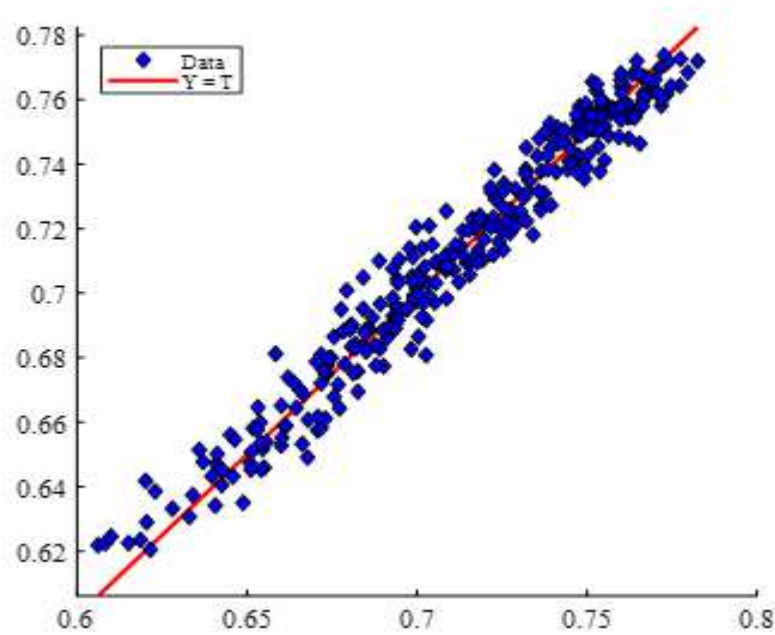
- 298 ➤ Y : Relative humidity value, calculated by the network (estimated value);
- 299 ➤ X : Row vector representing the row of inputs received by the network; it is the
300 vector representing the independent variables (meteorological parameters) ;
- 301 ➤ $\text{IW}_{1,1}$: Matrix of connection weights linking the input layer to the hidden layer;
- 302 ➤ $\text{LW}_{2,1}$: Matrix of connection weights linking the hidden layer to the output layer;
- 303 ➤ Tansig : Hidden Layer Activation Function;
- 304 ➤ Purelin : Output layer activation function;
- 305 ➤ θ_1 : Bias of the hidden layer;
- 306 ➤ θ_2 : Bias of the output layer.

307 The determination of the parameters of the model (essentially the connection weights and
308 prejudices) is performed according to a calculation algorithm. The purpose of this calculation
309 is the minimization of the error function (MSE) between the desired (observed) values and the
310 responses to the output of the model (estimated).

311 **III. 7** Performance evaluation of the established model

312 We tested the performance of our network with another performance indicator, which is the
313 schematic presentation of the values observed as a function of the estimated values. Figure 5

314 represents the relationship between the estimated values using a MLP type neural model of
315 configuration [5-11-1] and the values observed in the Rabat-Kenitra region.



316
317 **Fig. 5 :** Relationship between the estimated values (\hat{Y}) using a neural configuration model [5-11-1]
318 and the observed values (Y) in the Rabat-Kénitra region.

319 It clearly shows the predictive power of this model in predicting humidity levels in this
320 region. This performance is evaluated by a correlation coefficient ($R = 0.98$) for all the total
321 data. This predictive power developed by PMC type ANNs is in perfect agreement with the
322 results found by Smith and al. in 2006 for the prediction of air temperature [Vassiliki and al.,
323 2013], and those found in 2014 by El Badaoui and al., to predict the humidity rate in the
324 Chefchaouen region (Morocco) [Ben El Houari and al., 2014], as well as those found in 2015
325 by Ben El Houari et al. [Ben El Houari and al., 2016], concerning the forecast of the air
326 temperature of the city of Meknes (Morocco). These mathematical models developed by these
327 authors as well as our relevant model use a Levenberg-Marquardt type learning algorithm.

328 In addition, the correlation coefficient obtained by testing the validity of our model
329 established by the ANNs is much closer to that linked to learning. This shows a very good
330 correlation between the simulated and observed values with a very good correlation coefficient.
331 This proves the advantage of our predictive model established for the calculation of the relative
332 humidity rate in the Rabat-Kenitra region.

333 **IV. CONCLUSION**

334 As part of this study, we sought to develop an efficient mathematical model based on
335 artificial neuron networks, for the prediction of relative humidity rates, from meteorological
336 parameters of the region of Rabat-Kenitra.

337 To determine the most efficient and effective model, we studied the effects of the type of
338 artificial neural network, the number of neurons in the hidden layer, activation functions, the
339 learning algorithm on the efficiency of the developed mathematical model; and this by
340 calculating and comparing the correlation coefficients and the mean squared errors.

341 Thus, we have shown that the model based on artificial neuron networks of the PMC type,
342 of configuration [5-11-1], using a Levenberg-Marquardt learning algorithm with a nonlinear
343 activation function of the Tansig type in the hidden layer, and a linear activation function of the
344 Purelin type in the output layer, is the more efficient than the other models studied within the
345 framework of this study.

346 This performance of this model can be considered as an important tool, having a high
347 efficiency in the field of the prediction of relative humidity levels in the region of Rabat-
348 Kenitra.

349 -Ethical Approval: We do not need research data support or it is not applicable;

350 -Consent to Participate: All participants provided informed consent to participate and to
351 have the results disseminated in a variety of ways;

352 -Consent to Publish: Corresponding author: Abdelaziz ABDALLAOUI transfers to Springer
353 the non-exclusive publication rights and he warrants that his/her contribution is original and
354 that he/she has full power to make this grant. He signs for and accepts responsibility for
355 releasing this material on behalf of any and all co-authors. This transfer of publication rights
356 covers the non-exclusive right to reproduce and distribute the article, including reprints,
357 translations, photographic reproductions, microform, electronic form (offline, online) or any
358 other reproductions of similar nature (Cover letter).

359 -Authors Contributions:

360 ☞ Kaoutar EL AZHARI:

361  A - study design

362  B - data collection

363  C - statistical analysis

- 364  D - data interpretation
- 365  E - manuscript preparation
- 366  F - literature search

367 ☞ . Badreddine ABDALLAOUI:

- 368  A - statistical analysis
- 369  B - data interpretation
- 370  C-manuscript preparation

371 ☞ Ali DEHBII:

- 372  A - study design
- 373  B - manuscript preparation
- 374  C- literature search

375 ☞ Abdelaziz ABDALLAOUI:

- 376  A - study design
- 377  B - data collection
- 378  C - statistical analysis
- 379  D - data interpretation
- 380  E - manuscript preparation
- 381  F- literature search

382 ☞ Hamid ZINEDDINE:

- 383  A - study design
- 384  B - data interpretation
- 385  C - manuscript preparation
- 386  D- literature search

387 -Funding: This research received no specific grant from any funding agency in the public,
388 commercial, or not-for-profit sectors.

389 -Competing Interests: Personal financial interests and We do not consider diversified trusts
390 to constitute a competing financial interest.

391 -Availability of data and materials: Available.

392

393

Références

- 394 ▪ Abdallaoui A. & El Badaoui H., 2011. *Intelligences artificielles pour modéliser les*
395 *données météorologiques*. Éditions Universitaires Européennes. 216 p.
- 396 ▪ Abhishek K., Singh M. P., Ghosh S., Anand A., 2012. Weather forecasting model using
397 Artificial Neural Network, Computer Science and Engineering Department, NIT Patna,
398 Inde, Technology Process, vol. 4, 311 – 318.
- 399 ▪ Alayat H., El Badaoui H., Abdallaoui A., Abrid D., El Hmaidi A., 2018. Development
400 of mathematical models for predicting the iron concentrations of Lake Oubeira waters
401 (NE ALGERIAN). *J. Fundam. Appl. Sci.*, 2018, 10 (1), 83-96.
- 402 ▪ Ben El Houari M., Zegaoui O., Abdallaoui A., 2014. Development of Mathematical
403 Models to Forecasting The Monthly Precipitation, *American Journal of Engineering*
404 *Research (AJER)*, Volume 3, Issue 11, 38-45.
- 405 ▪ Ben El Houari M., Abdallaoui A., Zegaoui O., 2016. Forecasting of the ambient air
406 temperature using the artificial neural networks, *International Journal of Multi-*
407 *disciplinary Sciences (IJMS)*, Volume 3, Issue 2, 14-19.
- 408 ▪ Ben El Houari M., Zegaoui O., Abdallaoui A., 2015. Prediction of air temperature using
409 Multi-layer perceptrons with Levenberg-Marquardt training algorithm, *International*
410 *Research Journal of Engineering and Technology (IRJET)*, Volume 2, Issue 8, 26-32.
- 411 ▪ Ben El Houari M., Zegaoui O., Abdallaoui A., 2016. The use of Kohonen self-
412 organizing maps to study meteorological parameters in Meknes city (Morocco),
413 *International Journal of Scientific & Engineering Research (IJSER)*, Volume 7, Issue 7,
414 608-612.
- 415 ▪ Ben El Houari M., Zegaoui O., Abdallaoui A., 2016. Development of Multilayer
416 Perceptron and Radial Basis Function Artificial Neural Network models for forecasting
417 the monthly air temperature. *Advances in Information Technology: Theory and*
418 *Application*, 1 (1), 147-152.
- 419 ▪ Bimal D., Susanta M., 2011. Better Prediction of Humidity using Artificial Neural
420 Network, *Fourth International Conference on the Applications of Digital Information*
421 *and Web Technologies*. IEEE 59-64.
- 422 ▪ Bishop C. M., 1995. *Neural networks for pattern recognition*,” Oxford, Presse
423 universitaire, 498 p.
- 424 ▪ Dedecker A., Peter L., Goethals M., Gabriels W., De Pauw N., 2002. Optimisation of
425 Artificial Neural Network (ANN) model design for prediction of macroinvertebrate
426 communities in the Zwalm river basin (Flanders, Belgium). *The Scientific World*
427 *Journal*, 2, 96-104.
- 428 ▪ Dombayc O. A., Golcu M., 2009. Daily means ambient temperature prediction using
429 artificial: a case study of Turqy. *Energie renevlable*, 34, 1158-1161.
- 430 ▪ El Badaoui H., Abdallaoui A., Chabaa S., 2014. Multilayer Perceptron and Radial Basis
431 Function Grating for Moisture Prediction. *International Journal of Innovation and*
432 *Scientific Research*, volume 5 (1), 55-67.

- 433 ▪ El Azhari K., El Badaoui H., Abdallaoui A., Zineddine H., 2017. Optimization of neural
434 architectures for prediction of heavy metal concentrations in Red Sea sediments.
435 International Journal of Scientific & Engineering Research Volume 8, Issue 7, 906-912.
- 436 ▪ El Badaoui H., Abdallaoui A., Chabaa S., 2014. Using MLP neural networks for
437 predicting global solar radiation. The International Journal of Engineering and Science
438 (IJES), volume 2 (12), 15-26.
- 439 ▪ French, M. N., Krajewski, W. F., Cuykendal, R. R., 1992. Rainfall forecasting in space
440 and time using a neural network. Journal d'Hydrologie, 137, 1–37.
- 441 ▪ Gardner M. W., Dorling S. R., 1998. Artificial Neural Networks (the Multilayer
442 Perceptron)—A Review of Applications in the Atmospheric Sciences. Environnement
443 Atmosphérique, 32, 2627-2636.
- 444 ▪ Hsu, K., Gao X., Sorooshain, S., Gupta, H. V., 1997. Precipitation estimation from
445 remotely sensed information using artificial neural networks. Journal de météorologie
446 appliquée, 36(9), 1176–1190.
- 447 ▪ Hubbard, K. G., Mahmood R., Carlson C., 2003. Estimation of daily dew point
448 temperature in the northern Great Plains using maximum and minimum temperatures.
449 Agron. J., 95, 323-328.
- 450 ▪ Imran T., Shafiqur R., Khaled B., 2002. Application of neural networks for the
451 prediction of hourly mean surface temperatures in Saudi Arabia. Renewable Energy.
452 Vol 25, 545-554.
- 453 ▪ Kemajou A., Léopold MBA, Meukam P., 2012. Application of artificial neural network
454 for predicting the indoor air temperature in modern building in humid region. British
455 Journal of Applied Science & Technology. Vol 2 (1), 23-34.
- 456 ▪ Laafou S., Omari H., Abdallaoui A., 2016. Application of artificial neural networks with
457 error back-propagation algorithm to predict nitrate levels in water. Advances in
458 Information Technology: Theory and Application, 1 (1), 135-140.
- 459 ▪ Lu T., Viljanen M., 2009. Prediction of indoor temperature and relative humidity using
460 neural network models: model comparison. Journal de l'informatique neuronale et
461 applications. Vol 18, 345–357.
- 462 ▪ Luk, K. C., Ball J., Sharma A., 2000. A study of optimal model lag and spatial inputs to
463 artificial neural network for rainfall forecasting. Journal d'Hydrologie, 227, 56-65.
- 464 ▪ Mahmood, R., Hubbard K. G., 2005. Assessment of bias in estimates of
465 evapotranspiration and soil moisture through the use of modeled solar radiation and dew
466 point temperature data. Agriculture and forest Meteorology, 130, 71-84.
- 467 ▪ Omari H., Abdallaoui A., Laafou S., 2016. Multilayer perceptron neural networks with
468 error back-propagation algorithm for the prediction of nitrate concentrations in
469 groundwater. The International Journal of Multi-disciplinary Sciences, 3 (2), 1–7.
- 470 ▪ Parishwad G. V., Bhardwaj R. K., Nema V.K., 1998. Prediction of monthly-mean
471 hourly relative humidity, ambient temperature, and wind velocity for India. Renew
472 Energy. Vol 13(3), 363–380.
- 473 ▪ Radhika Y., Shashi M., 2009. Atmospheric Temperature Prediction using Support
474 Vector Machines,” International Journal of Computer Theory and Engineering, Vol. 1,
475 No. 1, 1793-8201.

- 476 ▪ Rojas R., 1996. Neural Networks. A Systematic Introduction. Springer-Verlag, Berlin,
477 509 p.
- 478 ▪ Santhosh Baboo S., Shereef I. K., 2010. An Efficient Weather Forecasting System using
479 Artificial Neural Network. International Journal of Environmental Science and
480 Development, Vol. 1, No. 4, ISSN: 2010-0264.
- 481 ▪ Smith, B. A., McClendon R. W., Hoogenboom G., 2006. Improving air
482 temperature prediction with artificial neural networks. Journal international
483 d'intelligence computationnelle, 3, 179-186.
- 484 ▪ Turkan G. Ö., Sezer A., Yıldız Y., 2012. Models for Prediction of Daily Mean Indoor
485 Temperature and Relative Humidity: Education Building in Izmir, Turkey. Indoor Built
486 Environ vol 21 (6), 772–781.
- 487 ▪ Trahi F., 2011. Prédiction de l'irradiation solaire globale pour la région de Tizi-Ouzou
488 par les réseaux de neurones artificiels. Application pour le dimensionnement d'une
489 installation photovoltaïque pour l'animation du laboratoire de recherche LAMPA,
490 Magister en électronique, Université de Tizi-Ouzou, 113 p.
- 491 ▪ Vassiliki Mantzari H., Dimitrios Mantzaris H., 2013. Solar radiation: Cloudiness
492 forecasting using a soft computing approach, Artificial Intelligence Research, volume
493 2, 69-80.

Figures

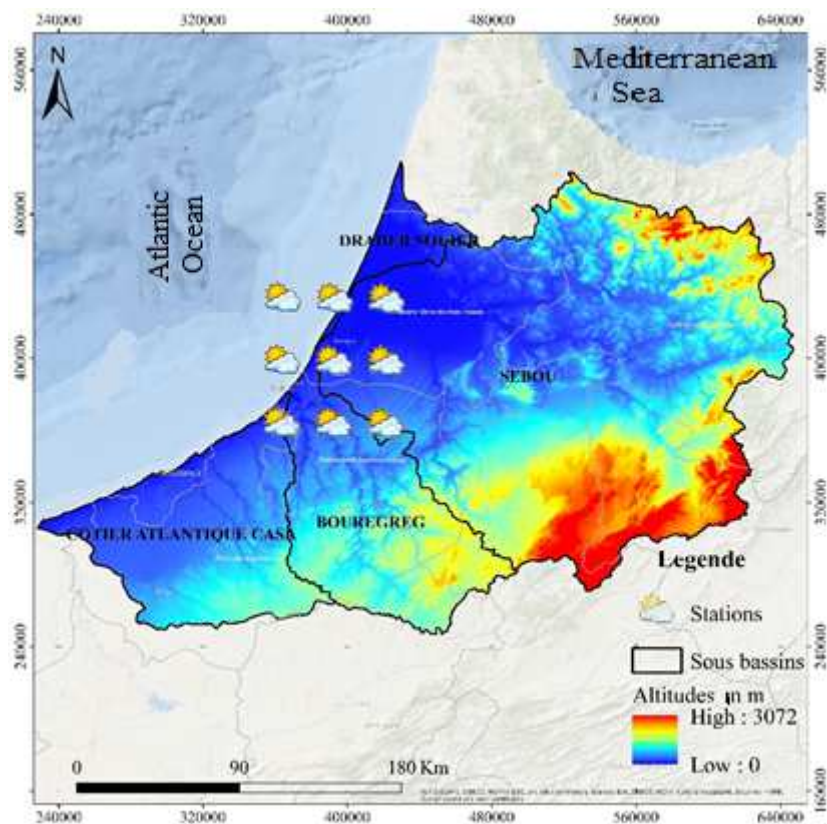


Figure 1

Map of meteorological stations location in the Rabat-Kenitra region (Morocco). Note: The designations employed and the presentation of the material on this map do not imply the expression of any opinion whatsoever on the part of Research Square concerning the legal status of any country, territory, city or area or of its authorities, or concerning the delimitation of its frontiers or boundaries. This map has been provided by the authors.

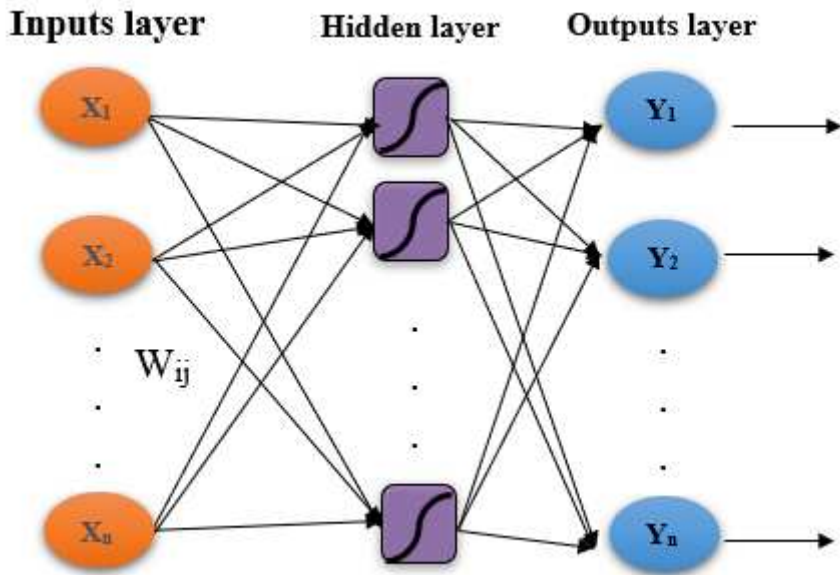


Figure 2

Architecture of a neural network with 3 layers.

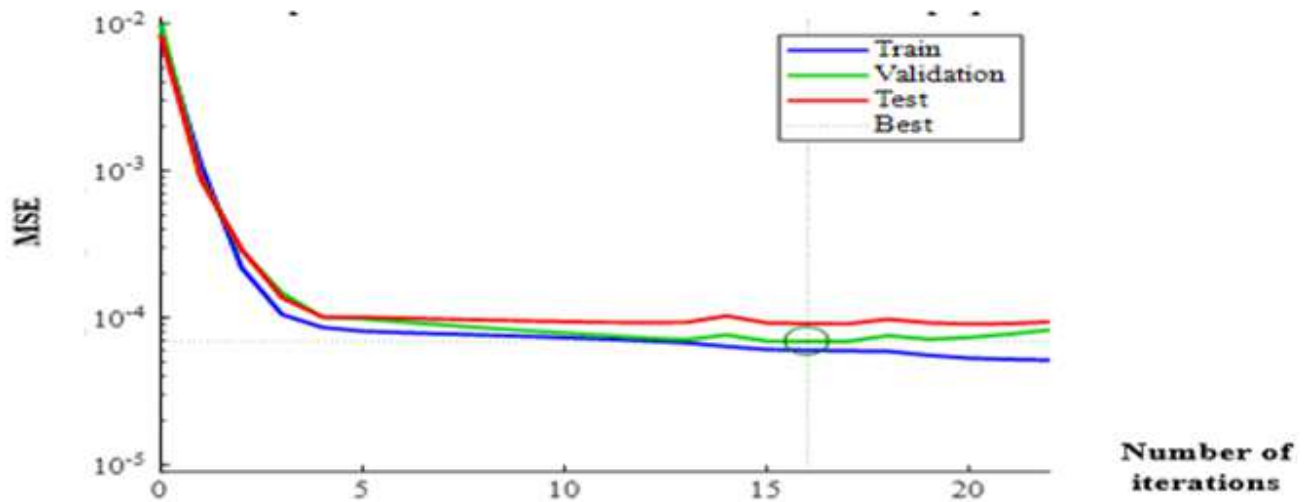


Figure 3

Evolution of average quadratic error with 11 neurons in the hidden layer.

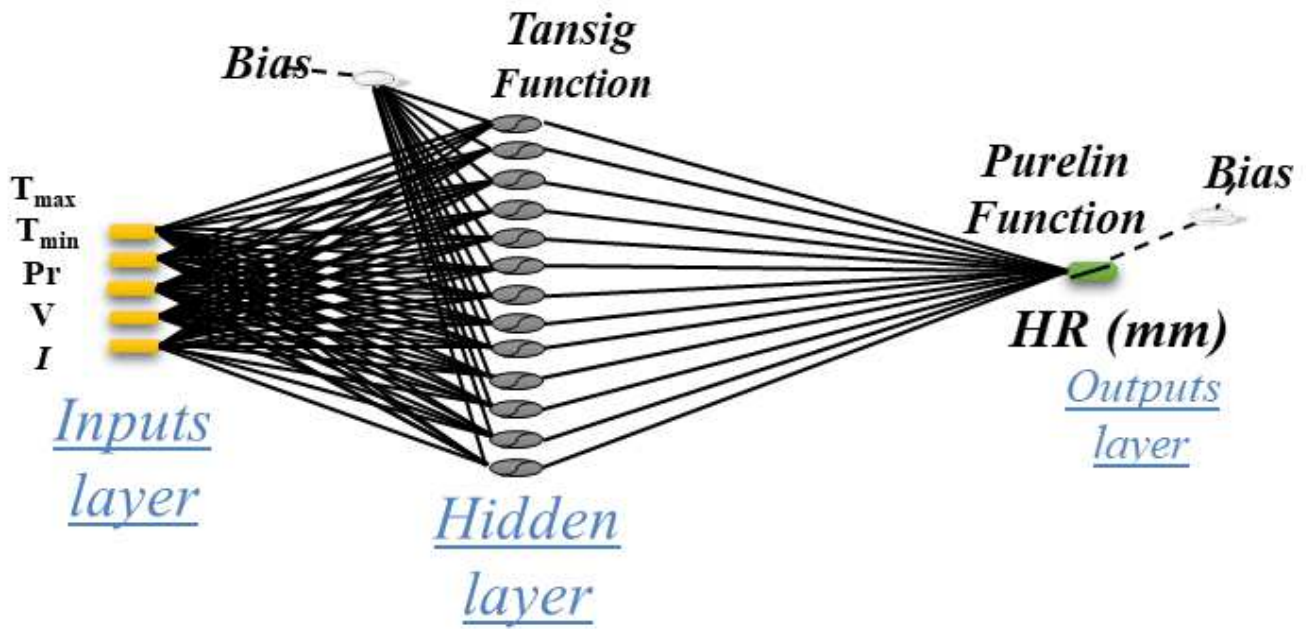


Figure 4

Architecture of the neural network with three configuration layers [5-11-1] developed for the prediction of relative humidity in the region of Rabat-Kenitra.

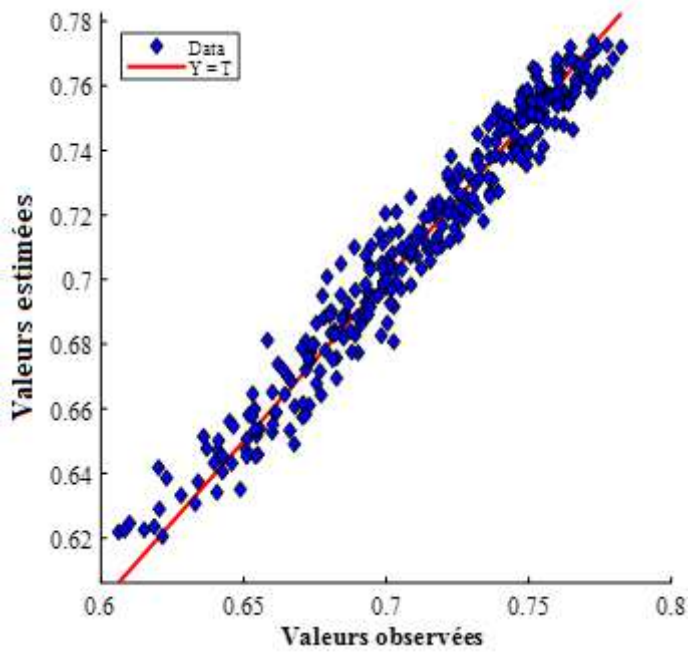


Figure 5

Relationship between the estimated values (\hat{Y}) using a neural configuration model [5-11-1] and the observed values (Y) in the Rabat-Kénitra region.